Free Energy of Transition for the Individual Alkaline Conformers of Yeast Iso-1-cytochrome *c*[†,‡]

Gianantonio Battistuzzi,[§] Marco Borsari,[§] Francesca De Rienzo,[§,||] Giulia Di Rocco,[§] Antonio Ranieri, and Marco Sola*[,§,||]

Department of Chemistry, University of Modena and Reggio Emilia, Via Campi 183, I-41100 Modena, Italy, and CNR-INFM National Center, Nanostructures and Biosystems at Surfaces−S3, Via Campi 213/A, I-41100 Modena, Italy

Received September 21, 2006; Revised Manuscript Received December 10, 2006

ABSTRACT: Direct protein electrochemistry was used to obtain the thermodynamic parameters of transition from the native (state III) to the alkaline (state IV) conformer for untrimethylated *Saccharomyces cerevisiae* iso-1-cytochrome *c* expressed in *E. coli* and its single and multiple lysine-depleted variants. In these variants, one or more of the lysine residues involved in axial Met substitution (Lys72, Lys73, and Lys79) was mutated to alanine. The aim of this work is to determine the thermodynamic affinity of each of the substituting lysines for the heme iron and evaluate the interplay of enthalpic and entropic factors. The equilibrium constants for the deprotonation reaction of Lys72, 73, and 79 were computed for the minimized MD average structures of the wild-type and mutated proteins, applying a modified Tanford−Kirkwood calculation. Solvent accessibility calculations for the substituting lysines in all variants were also performed. The transition enthalpy and entropy values within the protein series show a compensatory behavior, typical of a process involving extensive solvent reorganization effects. The experimental and theoretical data indicate that Lys72 most readily deprotonates and replaces M80 as the axial heme iron ligand, whereas Lys73 and Lys79 show comparably higher pK_a values and larger transition free energies. A good correlation is found within the series between the lowest calculated Lys pK_a value and the corresponding experimental pK_a value, which can be interpreted as indicative of the deprotonating lysine itself acting as the triggering group for the conformational transition. The triple Lys to Ala mutant, in which no lysine residues are available for heme iron binding, features transition thermodynamics consistent with a hydroxide ion replacing the axial methionine ligand.

Ferricytochrome *c* (cytc[1]) undergoes at least two reversible conformational transitions in the pH range 7−12, involving the replacement of the methionine residue axially bound to the heme iron (Met80) by a stronger ligand (*1*, *2*). This process, occurring at pH values above 8, is known as the "alkaline transition" and involves a lysine residue as a substituting ligand (*3*−*17*). Such a transition, due to the large decrease in reduction potential associated with the ligand exchange, may be implicated in the control of the electron transfer rate between cytochrome *c* and cytochrome *c* oxidase, thus playing a fundamental role in energy transduction, at least in eukaryotic cells (*4*). Moreover, the alkaline conformer of cytochrome *c* has been claimed to be involved in apoptosis, which is programmed cellular death (*18*−*23*). Even though alkaline transition has attracted considerable interest in the last three decades, the identity of the substituting ligand has been unequivocally determined only recently (*3*), and the detailed mechanism has as yet escaped clear definition. At present, the generally accepted minimal scheme is that of a two-step mechanism in which a fast residue deprotonation triggers a slow and thermodynamically favored conformational change involving axial ligand substitution (*15*, *16*, *24*−*27*). The overall reaction features a species-dependent apparent pK_a (pK_{app}) of approximately 8−9 (*1*, *2*).

The existence of at least two alkaline isomers in a pH-dependent ratio for all mitochondrial cytc suggested that at least two Lys residues can replace the methionine ligand at high pH (*4*−*6*, *9*, *12*). Recent studies on site-directed mutants of yeast iso-1 cytc indicated Lys79 and Lys73 as the iron ligands (*4*, *5*, *9*, *27*), whereas the most likely candidates in horse heart cytc are Lys79 and Lys72 (*4*, *5*, *8*). The thermodynamics of the transition have been previously determined for a number of cytochromes *c* through direct electrochemistry experiments carried out at varying pH and temperature values (*28*−*30*). Because of the existence of multiple substituting ligands, the data turn out to be weighted averages over the populations of each alkaline conformer.

[†] This work was supported by the Ministero dell'Universitá e della Ricerca Scientifica e Tecnologica of Italy (Programmi di Ricerca Scientifica di Rilevante Interesse Nazionale, PRIN 2003) and by the COST (Cooperation in the field of Scientific and Technical Research) D21 action of the European Community (WG D21/0011/01).

[‡] This work is dedicated to Maria Silvia Viezzoli, who passed away on August 31, 2005.

* To whom correspondence should be addressed. Tel: +39 059 2055037. Fax: +39 059 373543. E-mail: sola.marco@unimore.it.

[§] University of Modena and Reggio Emilia.

[||] CNR-INFM National Center.

[1] Abbreviations: cytc, untrimethylated iso-1-cytochrome *c* from *Saccharomyces cerevisiae*; ET, electron transfer; $\Delta H^{\circ\prime}_{AT}$, enthalpy change for the alkaline transition; $\Delta S^{\circ\prime}_{AT}$, entropy change for alkaline transition; SCE, saturated calomel electrode; SHE, standard hydrogen electrode.

10.1021/bi061961e CCC: $37.00
Published on Web 01/23/2007

Determining the contribution of each conformer to transition thermodynamics would allow the identification of the substituting Lys residue with the strongest metal binding affinity and the assessment of the interplay between enthalpic and entropic effects. To this end, exploiting the same electrochemical approach, here we have measured the transition thermodynamics for mutants of yeast iso-1 cytochrome *c* expressed in *E. coli* in which the lysine residues involved in the alkaline transition have been replaced by alanine residues. In particular, we have investigated all of the single (K72A, K73A, and K79A) and double (K72A/K73A, K72A/K79A, and K73A/K79A) mutants and also the triple mutant (K72A/K73A/K79A), which possesses no lysine with the ability to bind to the heme iron. Moreover, molecular dynamics (MD) simulations of the structures of the cytc mutants were performed to investigate the environment of the heme and of the remaining Lys residues, with particular focus on solvent accessibility. On the basis of this, the pK_a values for Lys72, 73, and 79 were computed by applying a modified Tanford−Kirkwood calculation. The thermodynamic experiments and the MD simulations indicate that Lys72 is the axial ligand originating the most stable alkaline conformer in the bacterially expressed yeast iso-1-cytc and that in each alkaline conformer, the binding lysine itself acts as the deprotonating group triggering the transition.

EXPERIMENTAL PROCEDURES

Protein Production and Isolation. Yeast iso-1 cytochrome c variants (K72A, K73A, K79A, K72A/K73A, K72A/79A, K73A/K79A, and K72A/K73A/K79A) were produced and purified following the procedure described elsewhere (*4*, *31*, *32*). Thr replaces Cys102 in all variants. This substitution prevents dimerization and minimizes autoreduction while resulting in retention of the spectral and functional properties of the protein (*33*, *34*). The QuikChange XL site-directed mutagenesis kit (Stratagene) was used for the Lys to Ala substitution starting from two synthetic oligonucleotide primers carrying the desired mutation and the plasmid pMSV1 that expresses the protein from the pTrc promotor and confers ampicillin resistance to the cells (*35*).

K72A F: 5′-CAGAGTACTTGACTAACCCAGCGAAATATATTCCTGGCACC-3′;

K72A R: 5′-GGTGCCAGGAATATATTTCGCTGGGTTAGTCAAGTACTCTG-3′;

K73A F: 5'-GAGTACTTGACTAACCCAAAGGCCTATATTCCTGGTACCAAGATG-3'

K73A R: 5'-CATCTTGGTACCAGGAATATAGGCCTTTGGGTTAGTCAAGTACTC-3'

K79A F2: 5'-GAAATATATTCCTGGTACCGCTATGGCCTTTGGTGGGTTG-3'

K79A R2: 5'-CAACCCACCAAAGGCCATAGCGGTACCAGGAATATATTTC-3'

K7273A F: 5'-GAGTACTTGACTAACCCAGCGGCCTATATTCCTGGTACCAAGATG-3'

K7273A R: 5'-CATCTTGGTACCAGGAATATAGGCCGCTGGGTTAGTCAAGTACTC-3'

The holoprotein was obtained by co-transformation of the plasmids containing the mutation and the pEC86 plasmid (kind gift of L. Thöny-Meyer, ETH Zurich, Switzerland) with the chloramphenicol marker, which expresses the *ccm* genes under the control of the tet promoter (*35*−*38*). Transformants were grown overnight in 30 mL of 2× YT medium containing 100 μg/mL ampicillin and 40 μg/mL chloramphenicol. The overnight precultures were used to inoculate 2 × 1.3 L of liquid 2× YT/Amp/Cam medium, into 2-L flasks. The overexpression of the protein was induced with 0.5 mM IPTG for 5 h (*35*). The protein was isolated through complete disruption of the cells by sonication and purified following the procedure reported by Pollock et al. (32). UV−visible absorption spectra were recorded with a Varian Cary 50 BIO spectrophotometer at 25 °C. Native and mutated proteins showed R_z values ($R_z = A_{410}/A_{280}$) in agreement with the literature value for the pure protein ($R_z > 4.5$) (*16*, *39*).

Electrochemical Measurements. Cyclic voltammetry experiments were carried out with a Potentiostat/Galvanostat PAR mod. 273A at different scan rates (0.02−1 V s^{-1}) using a cell for small volume samples (0.5 mL) under argon. A gold wire was used as the working electrode, and a Pt sheet and a saturated calomel electrode (SCE) as the counter and reference electrode, respectively. The electric contact between the SCE and the working solution was obtained with a Vycor set. Potentials were calibrated against the MV^{2+}/MV^{+} couple (MV = methyl viologen) (*40*, *41*). The working electrode was cleaned by heating it in KOH solution for 10 min and rinsing in water and then in concentrated sulfuric acid for 15 min. To minimize residual adsorbed impurities, the electrode was first set at +1 V (vs SCE) for 180 s and then subjected to 10 voltammetric cycles between +0.7 and −0.6 V at 0.1 V s^{-1}. The Vycor (PAR) set was treated in an ultrasonic pool for about 5 min. Modification of the electrode surface was performed by dipping the polished electrode into a 1 mM solution of 4-mercaptopyridine for 120 s and then rinsing it with MILLIQ water. Sodium chloride (0.1 M) was used as the base electrolyte. Protein solutions were freshly prepared before use in 10 mM phosphate buffer at pH 7 and 0.1 M NaCl, and their concentration, varying over 0.1 to 0.3 mM, was checked spectrophotometrically. The pH titrations at different temperatures were carried out with a "nonisothermal" cell (*28*, *29*) in which the reference electrode was kept at constant temperature (21 ± 0.1 °C), whereas the half-cell containing the working electrode and the Vycor junction to the reference electrode was under thermostatic control with a water bath. The temperature was varied from 10 to 35 °C. The pH was changed by adding small amounts of concentrated NaOH.

COMPUTATIONAL PROCEDURES

Refinement of the Protein 3D Structures. The crystal structure of *Saccharomyces cerevisiae* iso-1 cytochrome *c* used in the calculations was retrieved from the Protein Data Bank (pdb code: 1ycc) (http://www.rcsb.org/pdb/) (*42*). To simulate the protein expressed from *Escherichia coli*, the three-methylated Lys72 was changed to Lys and Cys102 to Thr. Moreover, the structures of the Lys to Ala mutants were produced through residue substitution carried out with the software package QUANTA 2000 (Molecular Simulation, Inc., Waltham, MA). Energy minimization and molecular dynamics (MD) calculations were performed with the program CHARMM (Harvard University) (43). The CHARMM24 united-atom force field and all-atom parameters were used for the proteins and the heme, respectively, together with a 15 Å nonbonded cutoff distance and a water dielectric constant of 80. The oxidized heme iron (with a formal charge of +3) was assigned a partial charge of +1.4 e (in agreement with previous calculations), and excess charge was distributed over the Fe-coordinating atoms, that is, the S atom of Met80, the Nϵ of His18, and the Ns of the

porphyrin. Energy minimization and MD procedures were performed as described by Manfredini et al. (*44*). Structure sampling was performed every 0.5 ps during the final 90 ps of each MD simulation. The average structures resulting from MD simulations were then minimized (*44*) and used for structural analysis, pK_a and solvent accessibility (SA) calculations, and evaluation of the interaction energies.

pK_a Calculations. The equilibrium constants for the deprotonation reaction of K72, K73, and K79 were computed for the minimized MD average structures of wild-type (wt) cytc and its mutants using the software MacroDox version 3.2.1 (http://pirn.chem.tntech.edu/) (*45*). This program computes the effective proton dissociation constants (pK_a) of the titratable residues by performing a surface-accessibility-modified Tanford−Kirkwood calculation, as described by Matthew and Gurd (*46*). In particular, intrinsic proton dissociation constants (based on pK_a values determined for model compounds) are first assigned to each titratable site in the protein. Then, the free energy of electrostatic interaction is calculated for each pair of charged sites on the protein surface, taking into account the burial depth of the titratable residues within the low-dielectric interior of the protein. This is done by calculating the surface accessibility (SA) of each formally charged atom of a titratable residue using Richard's surface algorithm with a solvent probe radius of 1.4 Å (*47*). The effective pK_a of each titratable residue is estimated iteratively, assuming that each protein charge distribution modifies the intrinsic pK_a assigned. The extent of this variation depends on the environmental conditions (pH, ionic strength, dielectric constant, and *T*). In our calculations, the experimental medium environment was simulated by setting the pH value to 7, the ionic strength to 0.1 M, the temperature to 298 K, and the solvent dielectric constant to 78.3. For the protein matrix, a mean dielectric constant of 20 was used (*48*). Standard MacroDox charges were used for the protein, whereas the heme iron was given a partial charge of +2, redistributing the remaining +1 charge on the Fe-coordinating atoms. To evaluate the error affecting the calculated effective pK_a values, the 180 structures sampled for the wild-type cytc during the MD run were clustered upon their rmsd values. A rmsd threshold cutoff of 0.95 was chosen, which corresponds to the maximum value of the rmsd Gaussian distribution. This clusterization procedure produced seven clusters. The lowest energy structure of each cluster was selected as representative of that group and was minimized with the same protocol used for the MD average structure. The minimized structures were then used to compute the pK_a values of the three studied lysines, following the same protocol described above. The average pK_a was computed for each of the three Lys residues. The variation of the calculated pK_a value of each Lys residue in the MD run turned out to be in the range of ±0.2 pH units, which was taken as the estimated error.

RESULTS

Transition Thermodynamics. As shown elsewhere (*16*, *28*−*30*), the intensity of the cathodic peak current of the voltammetric wave for the His−Met-ligated form (state III) of cytochrome *c* ($E^{\circ\prime}$ = +0.283 vs SHE at pH 7, T = 25 °C) remarkably decreases above pH 7 with a sigmoidal titration pattern due to the transition of native cytc to the alkaline conformer (state IV). The latter conformers originate

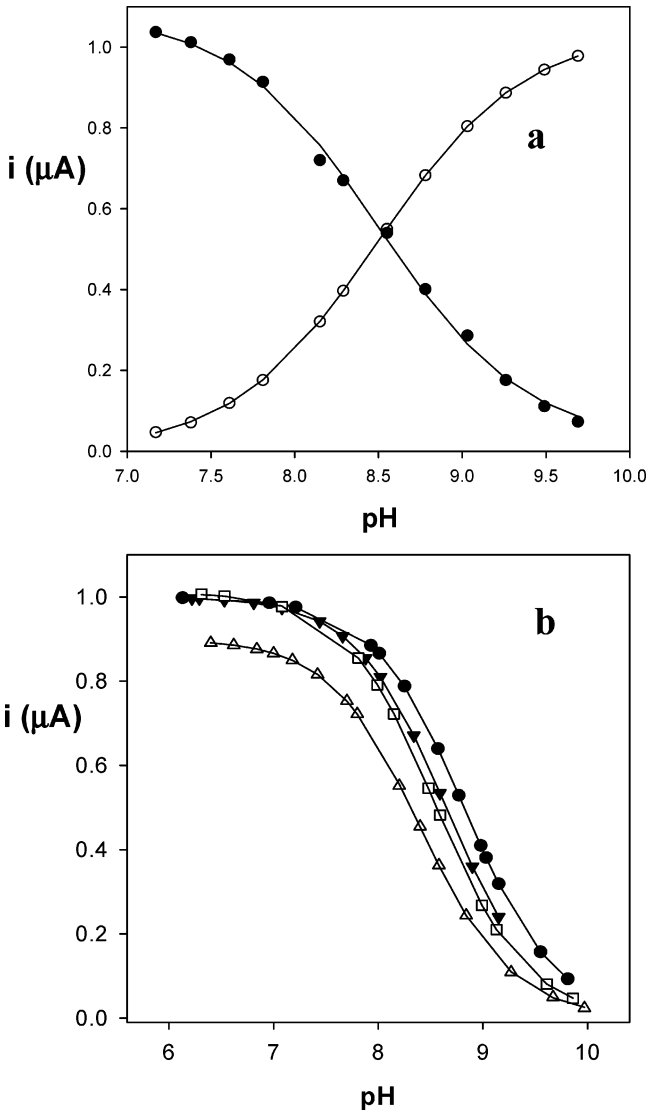

FIGURE 1: (a) pH dependence of the cathodic current intensity of the voltammetric signal for the native (state III) (●) and alkaline (state IV) (○) conformers of the K72AK73A variant of *Saccharomyces cerevisiae* iso-1 cytochrome *c* in 0.1 M sodium chloride, at T = 20 °C, and sweep rate = 0.05 V s^{-1}. (b) pH dependence of the cathodic current intensity for the native conformer (state III) of the K72A variant of *Saccharomyces cerevisiae* iso-1 K72A cytochrome *c* at different temperatures in 0.1 M sodium chloride: T = 10 (●), 20 (▼), 25 (□), 30 (△) °C; sweep rate = 0.05 V s^{-1}.

a single voltammetric signal at more negative potentials (E_{pc} = −0.205 vs SHE at pH above 7.5, T = 25 °C), whose intensity increases with increasing pH to the detriment of that of the native form, again featuring a sigmoidal behavior (an example is shown in Figure 1a). At each pH value and throughout the temperature range investigated, the cathodic currents of the voltammetric signals of the two conformers are independent of the scan rate in the range 0.02−1 V s^{-1}, indicating that the rate of heterogeneous electron transfer between the protein and the electrode is fast and that the current intensities are those determined by the chemical equilibrium between the two pH-dependent conformational states (*28*). Therefore, the apparent equilibrium constant (K_{app}) can be determined by fitting the current intensity values measured in the pH range 7−10 to a conventional one-proton equilibrium equation. The pK_{app} values obtained from the cathodic currents for the native and alkaline conformers are

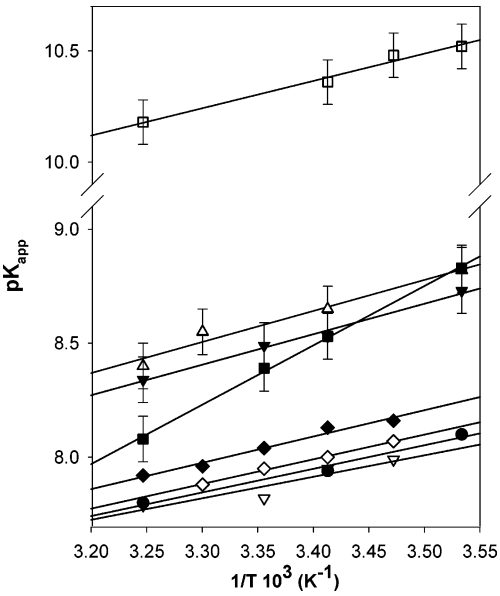

FIGURE 2: pK_{app} values for the alkaline transition of *Saccharomyces cerevisiae* iso-1 cytochrome *c* as a function of 1/*T* in 0.1 M sodium chloride. K73A (▽), wt C102T (●), K73A/K79A (◇), K79A (◆), K72A/K73A (▼), K72A/K79A (■), K72A (△); K72A/K73A/K79A (□). The solid lines are least-square fits to the data points.

Table 1: Thermodynamic Parameters for the Alkaline Transition (AT) of Native and Wild-Type Recombinant Untrimethylated *Saccharomyces cerevisiae* Iso-1-ferricytochrome *c* Expressed in *E. coli* and Its Lys to Ala Mutants[a]

species	$\Delta H^{\circ\prime}_{AT}$ (kJ mol^{-1})	$\Delta S^{\circ\prime}_{AT}$ (J mol^{-1} K^{-1})	$\Delta G^{\circ\prime}_{AT}$[b] (kJ mol^{-1})	pK_a[c]
wild type (C102T)	+20	−85	+45	7.9
K72A	+28	−69	+49	8.5
K73A	+18	−90	+45	7.8
K79A	+22	−80	+46	8.0
K72A/K73A	+26	−76	+48	8.5
K72A/K79A	+50	+7	+48	8.4
K73A/K79A	+20	−82	+45	8.0
K72A/K73A/K79A	+23	−118	+59	10.4
K73A[d]	+27	−79	+50	8.8
K79A[d]	+56	+24	+48	8.4
native[e]	+27	−72	+48	8.5

[a] The values were obtained in 10 mM phosphate buffer and 100 mM sodium chloride. The average errors on $\Delta H^{\circ\prime}_{AT}$ and $\Delta S^{\circ\prime}_{AT}$ values are ±2 kJ mol^{-1} and ±6 Jmol^{-1}K^{-1}, respectively. [b] Corresponding to the enthalpy change arising from transition-induced protein changes, $\Delta H^{\circ\prime}_{ATint}$ (see text); estimated error = ±0.3 kJ mol^{-1} (determined from the error affecting the pK_a values). [c] At 20 °C; estimated error = ±0.1 (upper value, determined from the standard deviation of the data set obtained from repeated pK_a measurements). [d] Recalculated from ref 4 (*4*). [e] Trimethylated native *Saccharomyces cerevisiae* iso-1-ferricytochrome *c* (from ref 29).

fully comparable and in good agreement with previous reports (*4*, *26*, *32*). In particular, the pK_{app} values for the three double mutants compare well with the microscopic pK_a values (8.0 ± 0.1, 8.35 ± 0.1, and 8.56 ± 0.05) determined for the untrimethylated bacterially expressed wt protein from pH titrations of the 695 nm charge-transfer band, although these titrations show hysteresis with regard to the direction of the titration (*26*). Transition thermodynamics ($\Delta H^{\circ\prime}_{AT}$ and $\Delta S^{\circ\prime}_{AT}$, where AT stands for alkaline transition) was evaluated by measuring the apparent equilibrium constants at varying temperature (from 10 to 35 °C) at $I = 0.1$ M (NaCl) (Figure 1b), using the integrated van't Hoff equation (under the hypothesis that $\Delta H^{\circ\prime}_{AT}$ is constant over the limited temperature range investigated), namely, from the plot of pK_{app} versus 1/*T* (eq 1) (28).

$$pK_{app} = \frac{\Delta H^{\circ\prime}_{AT}}{2.3R}\frac{1}{T} - \frac{\Delta S^{\circ\prime}_{AT}}{2.3R} \quad (1)$$

The van't Hoff plots for all of the species investigated are reported in Figure 2. The pK_{app} and the $\Delta S^{\circ\prime}_{AT}$ and $\Delta H^{\circ\prime}_{AT}$ values are listed in Table 1. Also listed are the values obtained by Mauk et al. using NMR for a few variants of yeast iso-1 cytochrome *c* (*4*), to facilitate discussion. Previous enthalpy values determined spectrophotometrically from the 695 nm absorption band for the native (trimethylated) and bacterially expressed (untrimethylated) protein differ from the present values by a factor of 2 (*26*). These differences could well arise from the different solution conditions because transition thermodynamics has been found to be very sensitive to ionic strength and solution composition (*28*).

Calculated pK_a Values. The effective pK_a values computed for the MD average structure of wt cytc and its Lys to Ala mutants are listed in Table 2. K72 shows the lowest pK_a value in wt cytc and mutants K73A and K79A, whereas K73 is the most readily deprotonating Lys in K72A. The lowest calculated pK_a for each mutant differs in general by about two units from the experimental pK_{app} values because of the different meanings of the two parameters. In fact, the former are the proton dissociation constants for the single Lys residues, whereas the latter are the apparent equilibrium constants of the overall reaction.

DISCUSSION

Transition Thermodynamics and Enthalpy−Entropy Compensation Phenomena. The alkaline transition in cytochrome *c* turns out to be disfavored both enthalpically (the reaction is endothermic) and entropically (in most cases, $\Delta S^{\circ\prime}_{AT}$ is negative) (Table 1). Thus, the reaction free energy ($\Delta G^{\circ\prime}_{AT}$) is positive for all of the species investigated. Because of the greater affinity of the lysine amino nitrogen for the ferric ion as compared to the methionine thioether sulfur, ligand substitution should not be responsible for the endothermicity of the process. Instead, this is likely to be determined by the deprotonation process and the transition-induced changes in the hydrogen-bonding network and the electrostatic interactions between the heme and the protein matrix (*28*, *29*). Changes in the conformational degrees of freedom of the polypeptide chain and, mostly, the solvent reorganization effects are the main contributors to reaction entropy, as discussed in more detail below.

Regarding the effects of charge changes upon mutation, pure electrostatic considerations suggest that the substitution of a positively charged lysine with a neutral alanine should disfavor deprotonation of the residue involved in the transition, with a consequent increase in the reaction enthalpy and free energy. This is the case for all mutants except K73A and K73A/K79A, whose parameters are comparable to those of wt cytc. However, we note that the increases in $\Delta H^{\circ\prime}_{AT}$ and $\Delta G^{\circ\prime}_{AT}$ correlate neither with the number of charge substitutions (i.e., $\Delta\Delta H^{\circ\prime}_{AT}$ and $\Delta\Delta G^{\circ\prime}_{AT}$ do not increase with increasing numbers of depleted lysines on passing from single to double mutants) nor with the distance of the substituted lysine residue(s) from the heme. This is not

Table 2: Calculated and Experimental pK_a Values for Untrimethylated *Saccharomyces cerevisiae* Cytochrome *c* Mutants Expressed in *E. coli*

S. cerevisiae iso−1 cytc mutant	calcd pK_a[a]			exp pK_{app}[b]	calcd pK_{app}[c]	Fe−ligand[d]	SA[e]			d(Nξ−Fe) Å[f]					
	K72	K73	K79				K72	K73	K79	K72		K73		K79	
C102T	10.1	10.9	11.3	7.9	7.9	K72	83.2	94.7	71.6	9.98	*0.34*	(10.0)	15.53	*0.32*	(15.8)	10.28	*0.20*	(9.93)
C102T/K72A		11.0	11.3	8.6	8.7	K73		96.0	61.3				15.74	*0.36*	(16.22)	10.32	*0.22*	(10.69)
C102T/K73A	10.2		11.1	7.8	8.0	K72	83.4		79.0	11.63	*0.62*	(12.6)				10.08	*0.27*	(9.65)
C102T/K79A	10.2	10.8		8.0	8.0	K72	63.7	76.3		10.05	*0.32*	(10.0)	16.00	*0.34*	(16.17)			
C102T/K72A/K73A			10.8	8.5	8.5	K79			61.1							9.85	*0.40*	(9.62)
C102T/K72A/K79A		10.6		8.4	8.3	K73		88.0					16.10	*0.33*	(16.31)			
C102T/K73A/K79A	10.2			8.0	8.0	K72	67.5			10.06	*0.30*	(10.0)						
C102T/K72A/K73A/K79A	n.d.	n.d.	n.d.	10.4	n.d.	none												

[a] The pK_a values for Lys 72, Lys73, and Lys79 were computed with the MacroDox program at $I = 100$ mM. The computed error is ±0.2. [b] The experimental pK_{app} values were electrochemically measured. The estimated error amounts to ±0.1. [c] Fitted pK_{app} values calculated with eq 2. [d] Suggested sixth Fe−ligand in the alkaline transition. [e] Solvent accessibility of the individual Lys residues (in Å^2) were computed with MacroDox. [f] MD average distance between the donor N_ξ atom of each Lys residue and the heme iron. The rms fluctuation about the average is reported in italics, whereas the d(Nξ−Fe) distance in the minimized average structure is provided in parenthesis.

FIGURE 3: Enthalpy−entropy compensation plot at 298 K for the thermodynamics of the alkaline transition for native, wt, and mutated *Saccharomyces cerevisiae* cytochrome *c*. Some values independently determined by Mauk et al. through MNR (*4*) are also added to the plot (□). The solid line represents the least-square fit to the data points ($R = 0.950$). The error bars have the same dimensions as that of the symbols. (○), K72A/K73A/K79A triple mutant.

surprising because the substitution of a surface lysine not only induces a charge effect, which is quenched by the dielectric properties of water, but also alters the population of the alkaline conformers, which feature nonequivalent reaction thermodynamics (*vide infra*).

We have demonstrated elsewhere that the reaction thermodynamics (either for the reduction or for the pH-induced conformational changes) for metalloproteins in aqueous solution is greatly affected by solvent reorganization phenomena (*28*−*30*, *49*−*51*). Therefore, the thermodynamic data listed in Table 1, as such, cannot be used to extract information on mutation-induced protein-based effects on transition thermodynamics. This is also the case for the present reaction series. In fact, it is worthy of note that for all of the present cytc variants (except for the triple mutant), the mutation-induced changes in $\Delta H^{\circ\prime}_{AT}$ and $\Delta S^{\circ\prime}_{AT}$ are much larger than the corresponding changes in $\Delta G^{\circ\prime}_{AT}$ (Table 1). This is typical of the presence of enthalpy−entropy compensation phenomena occurring within a series of homologous species subjected to the same reaction at fixed temperature (*29*, *49*−*51*). The compensation plot in which the entropic contributions to $\Delta G^{\circ\prime}_{AT}$ at 298 K ($T\Delta S^{\circ\prime}_{AT}$) are plotted against the corresponding enthalpic terms ($-\Delta H^{\circ\prime}_{AT}$) for all of the mutants investigated [also including the values determined by Mauk et al. through NMR for K73A and K79A cytc expressed in yeast (*4*)] is linear, with a slope close to unit, indicative of an almost exact compensation (Figure 3). As shown elsewhere (*49*−*51*), such an H−S compensation indicates that the reaction enthalpies and entropies for the individual reaction within the series are dominated by solvent reorganization effects due to transition-induced changes in the hydrogen-bonding network connecting the water molecules within the hydration sphere of the protein. These solvent reorganization effects, however, owing to perfect compensation, do not affect the reaction free energy. Therefore, $\Delta G^{\circ\prime}_{AT}$ is determined only by protein-based effects. If we assume, to a first approximation, that protein−based terms are minor contributors to the reaction

entropy, $\Delta G^{\circ\prime}_{AT}$ can be entirely assigned to enthalpy changes arising from intrinsic protein molecular changes, namely, $\Delta G^{\circ\prime}_{AT} = \Delta H^{\circ\prime}_{ATint}$ (*49*−*51*). In other words, the enthalpy change capturing the effects of transition-induced bonding formation/disruption within the protein is not the measured $\Delta H^{\circ\prime}_{AT}$ value, but it approximately corresponds to the reaction free energy change, $\Delta G^{\circ\prime}_{AT}$. The protein-based molecular factors involved include the deprotonation reaction, ligand substitution, and changes in the electrostatics at the interface among the heme, the protein, and the solvent (the latter as a bulk effect). Thus, any deviation from the perfect H−S compensation (which would imply a species-independent constant $\Delta G^{\circ\prime}_{AT}$ value), namely, any mutational change in $\Delta G^{\circ\prime}_{AT}$, must arise form the factors above. The assumption that protein-based entropic factors play a modest role in the reaction free energy is supported by the solution NMR structure of the alkaline conformer of the K72A/K79A variant (*3*), which shows the presence of a localized transition-induced protein conformational rearrangement occurring in close proximity of the heme. This structural modification occurs on the protein surface, thus most of the changes in the conformational degrees of freedom should be experienced by the network of H-bonded water molecules nearby.

The transition thermodynamics for the single mutants K72A, K73A, and K79A are the weighted averages of the parameters corresponding to the two alkaline conformers originated by the remaining lysine residues, the weighting factor being the molar fraction of each conformer. These mutants also provide information on how the removal of each individual lysine perturbs the system. In the double mutants, however, there is only one coordinating Lys residue, hence the transition thermodynamics is that of a single alkaline conformer (again perturbed with respect to the native protein by the removal of the other two lysines). We note that the thermodynamic parameters for the K72A variant are identical (within experimental error) to those for the native species in which Lys72 is trimethylated (*29*) (Table 1). This supports the reliability of the present data. In fact, in both cases, Lys72 is unavailable for Fe coordination. This result also suggests that the effect of lysine trimethylation is comparable to that of residue replacement with an alanine. In the same vein, the thermodynamics for the double mutants K72A/K73A and K72A/K79A is very similar to those for the K73A and K79A variants expressed in yeast (i.e., containing a trimethylated Lys72), obtained by Mauk et al. through NMR (*4*) (Table 1). The data for the single mutants indicate that the substitution of Lys72 is the one that perturbs the system more, rendering the transition enthalpically more disfavored ($\Delta G^{\circ\prime}_{AT}$ (= $\Delta H^{\circ\prime}_{ATint}$) increases from +45 to +49 kJ mol^{-1}). This finding indicates that the substitution of the axial ligand is more favored when Lys72 is available. This result is unequivocally supported by the data for the mutant K73A/K79A, in which K72 is the only binding lysine, which features the least positive $\Delta G^{\circ\prime}_{AT}$ (= $\Delta H^{\circ\prime}_{ATint}$) value. The other two double mutants show comparably higher transition free energies (Table 1). Thus, under the assumption that the lysine residues under consideration are electrostatically noninteracting (which is reasonable, considering that these are surface residues exposed to the solvent), we could conclude that Lys72 originates a more stable alkaline conformer with respect to Lys73 and Lys79. This result is in agreement with the evidence obtained by Mauk through ^{1}H NMR (*32*).

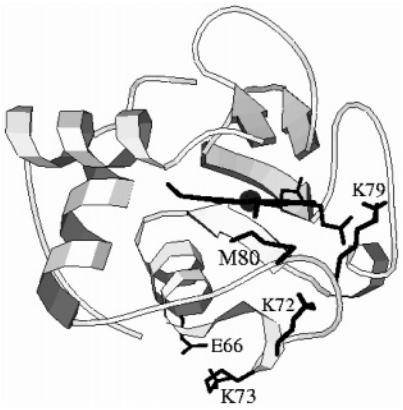

FIGURE 4: Three-dimensional representation of the averaged MD structure of *Saccharomyces cerevisiae* iso-1-cytochrome *c*. The ribbons describe α-helices and the arrows *β*-sheets. The heme is in sticks and the Fe in cpk. The mutated residues K72, K73, and K79, together with M80 and E66, are also shown in sticks.

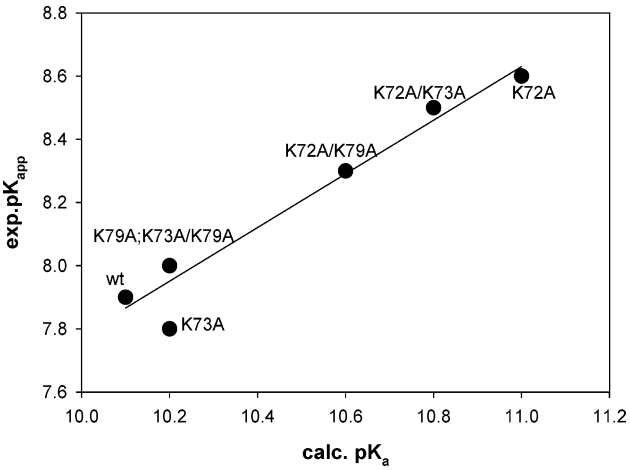

FIGURE 5: Plot of the lowest calculated pK_a value for each Lys to Ala variant of *Saccharomyces cerevisiae* iso-1 cytochrome *c* and the corresponding experimental pK_{app} value. The solid line represents the least-square fit to the data points (R = 0.966).

In the triple mutant (K72A/K73A/K79A), there are no lysines available for heme iron binding. The observed pK_{app} of 10.4 is higher by approximately two units than those for the other mutants. In this case, the protein most probably undergoes a transition from the native state III to state V, in which the axial Met80 residue is displaced by a hydroxide ion (*4*). Accordingly, the data point for this mutant falls off the compensation plot (Figure 3), indicating that the chemical event differs from that occurring within the series.

Calculated pKa Values for the Lys Residues. For all of the cytc variants under investigation, the calculated pK_a value for K72 is significantly lower than those for K73 and K79, which are almost identical (Table 2). Interestingly, the lowest calculated pK_a value and the corresponding experimental pK_a value for each mutant are linearly correlated within the series (Figure 5), according to the relationship

$$\exp \mathrm{p}K_{app} = 0.8698 \text{ calc } \mathrm{p}K_a - 0.9119 \qquad (2)$$

(with R = 0.966 and n = 7). The pK_{app} values predicted with this equation (calc pK_{app}), also listed in Table 2, are good estimates of the experimental data, considering experi-

mental error. This correlation indicates that the differences between the deprotonation constant of the most acidic lysine within the series closely parallel the differences in the experimental pK_{app} values. This observation has to do with the nature of the deprotonating group triggering ligand substitution. In fact, if we refer to the minimal two-step scheme for the transition, the most obvious explanation for this effect would be that the triggering group is the most acidic lysine itself (the deviation from unit slope might be related to the fact that the experimental pK_{app} values are weighted averages over the population of the various alkaline conformers) (*4*). This would imply that the subsequent step involving ligand exchange has the same equilibrium constant in all variants, simply determined by the balance between the two bond enthalpies (i.e., Lys(NH_2)-Fe vs Met(SCH_3)-Fe). This is in apparent conflict with the different extent of conformational change, involving the modification of hydrogen-bonding networks and other weak interactions, needed to bring each of the three different lysines at a bonding distance to the heme, which should affect the transition thermodynamics (*4*, *31*). However, the two views can be reconciled if we hypothesize that the conformational changes of the deprotonated surface lysines (i.e., bearing a neutral amino group), which must involve water molecules at the protein surface, contribute to the transition-induced enthalpy changes due to H-bonding reorganization within the hydration sphere of the molecule, which, as such, implies the presence of an exactly compensative entropic effect, thus not affecting the measured $\Delta G^{\circ\prime}_{AT}$ ($= \Delta H^{\circ\prime}_{ATint}$) value. The latter would, therefore, be ultimately determined mostly by residue deprotonation and heme Fe−ligand bond breaking/formation processes.

Structural Analysis. The minimized average MD structure of *Saccharomyces cerevisiae* iso-1-cytochrome *c*, with residues K72, K73, and K79 highlighted, is shown in Figure 4. The average distances between the amino nitrogen N_ζ of the Lys side chain and the heme Fe observed during the MD runs are summarized in Table 2. In all variants, K73 features the largest N_ζ−Fe distance (from 15.5 to 16.1 Å) and K79 the lowest (from 9.8 to 10.3 Å), whereas that for K72 is intermediate and covers a much wider range (from 10.0 to 11.6 Å). Interestingly, K72 also show rms fluctuations about the d(N_ζ−Fe) average value (reported in italics in Table 2), which are larger than K79 and comparable to K73. Thus, it seems that the Lys residue originating the most thermodynamically favored transition is not the one closest to the heme iron but that showing the most pronounced positional variability. Similarly, in the minimized MD average protein structures, K73 shows the largest solvent accessibility (SA) among the three studied lysines, followed by K72, which has a variable SA, and K79, which is the most buried (Table 2). In particular, the SA of K73 ranges between 76 and 96 $Å^2$ (15−20% of which is due to the side chain cationic head -NH_3^+), that of K72 varies between 63.7 and 83.4 $Å^2$, and that of K79 is between 61 and 79 $Å^2$ (involving only a minor contribution from the NH_3^+ group, with an upper figure of 5%). The limited solvent exposure and positional variability of the amino group of K79 are likely due to its involvement in a persistent extended H-bond network, which mainly involves a heme propionate, a nearby Thr residue (T49) and a few backbone carbonyl groups, with a resulting H-bond interaction energy (IE_{hbond}) ranging between −5.5 and −9.5 kcal/mol. This interaction network obstructs the ionization of the cationic head of K79 and consequently raises its pK_a by about one unit from its intrinsic reference value (10.4). The side-chain amino group of K73 features a IE_{hbond} from −5.8 to −7.2 kcal/mol, of which more than 50% is due to the interaction with E66. Although this value is lower than that for the amino group of K79, it might prevent K73 from being deprotonated at a pH lower than 10.6. Finally, K72 makes a few H-bonding interactions with nearby carbonyl groups, resulting in a IE_{hbond} between −6 and −6.7 kcal/mol. The interaction network involving K72 is less persistent during MD than those observed for K73 and K79 and allows greater mobility to K72. As a result, K72 appears to be the residue that can deprotonate more easily, in agreement with the above pK_a calculations. Moreover, the detailed analysis of the MD runs performed reveals that K72 points its side chain toward the interior of the protein, in the direction of the heme plane, whereas those of the other two residues protrude from the surface toward the solvent, maintaining their orientation thanks to the persistent H-bonds formed with the nearby residues (as discussed above). Thus, the conformational energy barrier for K72 coordination to the heme iron is likely to be the lowest among the three lysines. Whether this constitutes a factor that influences the thermodynamics of transition (*4*) or the kinetic barriers (the rate constant for the alkaline transition differs for the various Lys ligands (*4*)) cannot be said at the moment, although the present results would support the latter hypothesis.

CONCLUSIONS

The experimental and theoretical data presented here indicate that (i) K72 is the lysine residue that most readily deprotonates and replaces M80 as the axial heme iron ligand at alkaline pH values in recombinant yeast iso-1 cytochrome *c* expressed in *E. coli*; thus, the corresponding alkaline conformer prevails over the other two featuring K73 and K79 as the axial heme ligand; the population of the latter conformers may increase to some extent at higher pH values. (ii) When K72 is not available (i.e., deleted by mutation or trimethylated), K73 and K79 show comparable acid−base and coordinating abilities, although K73 from the theoretical analysis seems to be slightly favored. Thus, the capability of the three lysines to replace the axial methionine ligand to the heme iron follows the order K72 > K73 ≥ K79. This result is consistent with the conclusions drawn by Mauk on the basis of NMR data (*4*, *32*). From the relationship between the experimental and calculated pK_a values and from the MD and structural investigations, it is hypothesized that the conformational change subsequent to residue deprotonation and involving Lys for Met substitution does not contribute to the differences in the transition thermodynamics for the different substituting lysines, which instead appear to be controlled by the deprotonating ability of the lysine residue itself.

ACKNOWLEDGMENT

The plasmid pMSV used to obtain the mutated proteins was kindly donated by Professor Maria Silvia Viezzoli of the CERM and the Department of Chemistry of the University of Florence.

REFERENCES

1. Moore, G. R., and Pettigrew, G. W. (1990) *Cytochromes c. Evolutionary, Structural, and Physicochemical Aspects*, Springer-Verlag, Berlin, Germany.
2. Wilson, M. T., and Greenwood, C. (1996) In *Cytochrome c: A Multidisciplinary Approach* (Scott R. A., and Mauk, A. G., Eds.) Chapter 19, University Science Books, Sausalito, CA.
3. Assfalg, M., Bertini, I., Dolfi, A., Turano, P., Mauk, A. G., Rosell, F. I., and Gray, H. B. (2003) Structural model for an alkaline form of ferricytochrome *c*, *J. Am. Chem. Soc. 125*, 2913−2922.
4. Rosell, F. I., Ferrer, J. C., and Mauk, A. G. (1998) Proton-linked conformational switching: definition of the alkaline conformational transition of yeast iso-1 ferricytochrome c, *J. Am. Chem. Soc. 120*, 11234−11245.
5. Döpner, S., Hildebrandt, P., Rosell, F. I., and Mauk, A. G. (1998) Alkaline conformational transitions of ferricytochrome *c* studied by resonance Raman spectroscopy, *J. Am. Chem. Soc. 120*, 11246−11255.
6. Rosell, F. I., Harris, T. R., Hildebrand, D. P., Döpner, S., Hildebrand, P., and Mauk, A. G. (2000) Characterization of an alkaline transition intermediate stabilized in the Phe82Trp variant of yeast iso-1 cytochrome *c*, *Biochemistry 39*, 8054−9047.
7. Taler, G., Schejter, A., Navon, G., Vig, I., and Margoliash, E. (1995) The nature of the thermal equilibrium affecting the iron coordination of ferric cytochrome *c*, *Biochemistry 34*, 14209−14212.
8. Theodorakis, J. L., Garber, E. A. E., McCracken, J., Peisach Schejter, J. A., and Margoliash, E. (1995) Chemical modification of cytochrome-c lysines leading to changes in heme iron ligation, *Biochim. Biophys. Acta 1252*, 103−113.
9. Ferrer, J. C., Guillemette, J. G., Bogumil, R., Inglis, S. C., Smith, M., and Mauk, A. G. (1993) Identification of Lys79 as an iron ligand in one form of alkaline yeast iso-1 cytochrome *c*, *J. Am. Chem. Soc. 115*, 7507−7508.
10. Banci, L., Bertini, I., Spyroulias, G. A., and Turano, P. (1998) The conformational flexibility of oxidized cytochrome *c* studied through its interaction with NH_3 and high temperatures, *Eur. J. Inorg. Chem.* 583−591.
11. Wooten, J. B., Cohen, J. S., Vig, I., and Schejter, A. (1981) pH-induced conformational transitions of ferricytochrome c: a carbon-13 and deuterium nuclear magnetic resonance study, *Biochemistry 20*, 5394−5402.
12. Hong, X., and Dixon, D. W. (1989) NMR study of the alkaline isomerization of ferricytochrome *c*, *FEBS Lett. 246*, 105−108.
13. Gadsby, P. M. A., Peterson, J., Foote, N., Greenwood, C., and Thomson, A. J. (1987) Identification of the ligand-exchange process in the alkaline transition of horse heart cytochrome *c*, *Biochem. J. 246*, 43−54.
14. Ubbink, M., Campos, A. P., Teixeira, M., Hunt, N. I., Hill, H. A. O., and Canters, G. W. (1994) Characterization of mutant Met100Lys of cytochrome c-550 from *Thiobacillus versutus* with lysine-histidine heme ligation, *Biochemistry 33*, 10051−10059.
15. Lambeth, D. O., Campbell, K. L., Zand, R., and Palmer, G. (1973) The appearance of transient species of cytochrome *c* upon rapid oxidation or reduction at alkaline pH, *J. Biol. Chem. 248*, 8130−8136.
16. Barker, P. D., and Mauk, A. G. (1992) pH-linked conformational regulation of a metallo protein oxidation-reduction equilibrium: electrochemical analysis of the alkaline form of cytochrome *c*, *J. Am. Chem. Soc. 114*, 3619−3624.
17. Saraiva, L. M., Thomson, A. J., Le Brun, N. E., Liu, M.-Y., Payne, W. J., LeGall, J., and Moura, I. (1994) Replacement of methionine as the axial ligand of *Achromobacter cycloclastes* cytochrome c_{554} at high pH values revealed by absorption, EPR and MCD spectroscopy, *Biochem. Biophys. Res. Commun. 204*, 120−128.
18. Kluck, R. M., Bossy-Wetzel, E., Green, D. R., and Newmayer, D. D. (1997) The release of cytochrome c from mitochondria: a primary site for Bcl-2 regulation of apoptosis, *Science 275* 1132−1136.
19. Jang, X., and Wang, X. (2004) Cytochrome c mediated apoptosis, *Annu. Rev. Biochem. 73*, 87−106.
20. Degli Esposti, M. (2004) Mitochondria in apoptosis: past, present and future, *Biochem. Soc. Trans. 32*, 493−495.
21. Liu, X., Kim, C. N., Yang, J., Jemmerson, R., and Wang, X. (1996) Induction of apoptotic program in cell-free extracts: requirements for dATP and cytochrome *c*, *Cell 86*, 147−157.
22. Yang, J., Liu, X., Bhalla, K., Kim, C. N., Ibrado, A. M., Cai, J., Peng, T. I., Jones, D. P., and Wang, X. (1997) Prevention of apoptosis by Bcl-2: release of cytochrome c from mitochondria blocked, *Science 275*, 1129−1132.
23. Kluck, R. M., Martin, S. J., Hoffman, B. M., Zhou, J. S., Green, D. R., and Newmayer, D. D. (1997) The release of cytochrome c from mitochondria: a primary site for Bcl-2 regulation of apoptosis, *EMBO J. 16*, 4639−4649.
24. Davis, L. A., Schejter, A., and Hess, G. P. (1974) Alkaline isomerization of oxidized cytochrome c: equilibrium and kinetic measurements, *J. Biol. Chem. 249*, 2624−2632.
25. Kihara, H., Saigo, S., Nakatani, H., Hiromi, K., Ikeda-Saito, M., and Iizuka, T. (1976) Kinetic study of isomerization of ferricytochrome *c* at alkaline pH, *Biochim. Biophys. Acta 430*, 225−243.
26. Blouin, C., Guillemette, J. G., and Wallace, C. J. A. (2001) Resolving the individual components of a pH-induced conformational change, *Biophys J. 81*, 2331−2338.
27. Berghuis, A. M., and Brayer, G. D. (1992) Oxidation state-dependent conformational changes in cytochrome *c*, *J. Mol. Biol. 223*, 959−976.
28. Battistuzzi, G., Borsari, M., Loschi, L., Martinelli, A., and Sola, M. (1999) Thermodynamics of the alkaline transition of cytochrome *c*, *Biochemistry 38*, 7900−7907.
29. Battistuzzi, G., Borsari, M., Ranieri, A., and Sola, M. (2002) Conservation of the free energy change of the alkaline isomerization in mitochondrial and bacterial cytochromes *c*, *Arch. Biochem. Biophys. 404*, 227−233.
30. Battistuzzi, G., Borsari, M., and Sola, M. (2001) Medium and temperature effects on the redox chemistry of cytochrome *c*, *Eur. J. Inorg. Chem.* 2989−3004.
31. Northrup, S. H., Thomasson, K. A., Miller, C. M., Barker, P. D., Eltis, E. D., Guillemette, J. G., Inglis, S. V., and Mauk, A. G. (1993) Effects of charged amino acid mutations on the bimolecular kinetics of reduction of yeast iso-1-ferricytochrome c by bovine ferrocytochrome b_5, *Biochemistry 32*, 6613−6623.
32. Pollock, W. B. R., Rosell, F. I., Twitchett, M. B., Dumont, M. E., and Mauk, A. G. (1998) Bacterial expression of a mitochondrial cytochrome *c*. Trimethylation of Ly72 in yeast iso-1 cytochrome *c* and the alkaline conformational transition, *Biochemistry 37*, 6124−6131.
33. Cutler, R. J., Pielak, G. J., Mauk, A. G., and Smith, M. (1987) Replacement of cysteine-107 of *Saccharomyces cerevisiae* iso-1-cytochrome c with threonine: improved stability of the mutant protein, *Protein Eng. 1*, 95−99.
34. Liang, N., Mauk, A. G., Pielak, G. L., Johnson, J. A., Smith, M., and Hoffmann, B. (1988) Regulation of interprotein electron transfer by residue 82 of yeast cytochrome *c*, *Science 240*, 311−313.
35. Barker, T. D., Bertini, I., Del Conte, R., Ferguson, S. J., Hajieva, P., Tomlinson, E., Turano, P., and Viezzoli, M. S. (2001) A further clue to understanding the mobility of mitochondrial yeast cytochrome *c*, *Eur. J. Biochem. 268*, 4468−4476.
36. Arslan, E., Schulz, H., Zufferey, R., Künzler, P., and Thöny-Meyer, L. (1998) Overproduction of the *Bradyrhizobium japonicum* c-type cytochrome subunits of the cbb3 oxidase in *Escherichia coli*, *Biochem. Biophys. Res. Commun. 251*, 744−747.
37. Thöny-Meyer, L. (1997) Biogenesis of respiratory cytochromes in bacteria, *Microbiol. Rev. 61*, 337−376.
38. Schulz, H., Hennecke, H., and Thöny-Meyer, L. (1998) Prototype of a heme chaperone essential for cytochrome c maturation, *Science 281*, 1197−1200.
39. Margoliash, E., and Frohwirt, N. (1959) Spectrum of horse-heart cytochrome *c*, *Biochem. J. 71*, 570.
40. Battistuzzi, G., Borsari, M., Sola, M., and Francia, F. (1997) Redox thermodynamics of the native and alkaline forms of eukaryotic and bacterial class I cytochromes *c*, *Biochemistry 36*, 16247−16258.
41. Battistuzzi, G., Borsari, M., Cowan, J. A., Eicken, C., Loschi, L., and Sola, M. (1999) Redox chemistry and acid-base equilibria of mitochondrial plant cytochromes *c*, *Biochemistry 38*, 5553−5562.
42. Louie, G. V., and Brayer, G. D. (1990) High-resolution refinement of yeast iso-1-cytochrome c and comparisons with other eukaryotic cytochromes *c*, *J. Mol. Biol. 214*, 527−555.
43. Brooks, B. R., Bruccoleri, R. E., Olafson, B. D., States, D. J., Swaminathan, S., and Karplus, M. (1983) CHARMM: A program

for macromolecular energy, minimization, and dynamics calculations, *J. Comput. Chem. 4*, 187−217.
44. Manfredini, R., Tenedini, E., Siena, M., Tagliafico, E, Montanari, M., Grande, A., Zanocco-Marani, T., Poligani, C., Zini, R., Gemelli, C., Bergamaschi, A., Vignudelli, T., De Rienzo, F., De Benedetti, P. G., Menziani, M. C., and Ferrari, S. (2003) Development of an IL-6 antagonist peptide that induces apoptosis in 7TD1 cells, *Peptides 24*, 1207−1220.
45. Northrup, S. H. (1996) *MacroDox*, Version 2.0.2, Software for the prediction of macromolecular interactions, Tennessee Technological University, Cookeville, TN.
46. Matthew, J. B., and Gurd, F. R. N. (1986) Stabilization and destabilization of protein structure by charge interactions, *Methods Enzymol. 130*, 413−436.
47. Lee, B. K., and Richards, F. M. (1971) The interpretation of protein structures: estimation of static accessibility, *J. Mol. Biol. 55*, 379−400.
48. Antosiewicz, J., McCammon, J. A., and Gilson, M. K. (1994) Prediction of pH-dependent properties of proteins, *J. Mol. Biol. 238*, 415−436.
49. Battistuzzi, G., Borsari, M., Di Rocco, G., Ranieri, A., and Sola, M. (2004) Enthalpy/entropy compensation phenomena in the reduction thermodynamics of electron transport metalloproteins, *J. Biol. Inorg. Chem. 9*, 23−26.
50. Battistuzzi, G., Borsari, M., Ranieri, A., and Sola, M. (2004) Solvent-based deuterium isotope effects on the redox thermodynamics of cytochrome *c*, *J. Biol. Inorg. Chem. 9*, 781−787.
51. Battistuzzi, G., Borsari, M., Di Rocco, G., Leonardi, A., Ranieri, A., and Sola, M. (2005) Electrostatic effects on the thermodynamics of protonation of reduced plastocyanin, *ChemBioChem 6*, 692−696.

BI061961E